Europe PMC Funders Group
Author Manuscript
J Dermatol Sci. Author manuscript; available in PMC 2015 July 01.

Published in final edited form as:
J Dermatol Sci. 2015 July ; 79(1): 50–56. doi:10.1016/j.jdermsci.2015.03.019.

Connexin 43 deficiency accelerates skin wound healing and extracellular matrix remodeling in mice

Bruno Cogliati[#a,*], **Mathieu Vinken**[#b], **Tereza C. Silva**[a], **Cintia M.M. Araújo**[a], **Thiago P.A. Aloia**[a], **Lucas M. Chaible**[a], **Cláudia M.C. Mori**[a], and **Maria L.Z. Dagli**[a]

[a]Department of Pathology, School of Veterinary Medicine and Animal Science, University of São Paulo (USP), Brazil

[b]Department of In Vitro Toxicology and Dermato-Cosmetology, Vrije Universiteit Brussel (VUB), Brussels, Belgium

[#] These authors contributed equally to this work.

Abstract

Background—Cellular channels composed of connexin 43 are known to act as key players in the life cycle of the skin and consequently to underlie skin repair.

Objective—This study was specifically set up to investigate the suite of molecular mechanisms driven by connexin 43-based channels on wound healing.

Methods—To this end, a battery of parameters, including re-epithelialization, neovascularization, collagen deposition and extracellular matrix remodeling, was monitored over time during experimentally induced skin repair in heterozygous connexin 43 knockout mice.

Results—It was found that connexin 43 deficiency accelerates re-epithelialization and wound closure, increases proliferation and activation of dermal fibroblasts, and enhances the expression of extracellular matrix remodeling mediators.

Conclusion—These data substantiate the notion that connexin 43 may represent an interesting therapeutic target in dermal wound healing.

Keywords

Connexin 43; Gap junction; Skin repair; Wound healing

1. Introduction

Intercellular communication mediated by gap junctions is major driver of skin differentiation and remodeling. Gap junctions consist of 2 hemichannels of adjacent cells, which in turn are built up by 6 connexin (Cx) proteins. As many as 10 different connexin family members have been identified in human and rodent skin, all of which are named after

© 2015 Japanese Society for Investigative Dermatology. Published by Elsevier Ireland Ltd. All rights reserved.

[*]Corresponding author at: University of São Paulo, School of Veterinary Medicine and Animal Science, Department of Pathology, Av. Prof. Dr. Orlando Marques de Paiva, 87, Cidade Universitária, 05508-270 São Paulo, Brazil. Tel.: +55 11 30 91 12 00; fax: +55 11 30 91 78 29. bcogliati@usp.br (B. Cogliati) .

Europe PMC Funders Author Manuscripts
Europe PMC Funders Author Manuscripts

Europe PMC Funders Author Manuscripts

Europe PMC Funders Author Manuscripts

their molecular weight and are expressed in a cell type-specific and developmental stage-specific way [1–4]. Thus, keratinocytes in the epidermal *stratum basale* and *stratum spinosum* as well as dermal fibroblasts and endothelial cells abundantly express Cx43, while keratinocytes in the *stratum granulosum* mainly produce Cx26. Not surprisingly, connexin expression in the epidermis undergoes drastic modifications during skin repair and disease [5,6]. In fact, epidermal Cx43 expression decreases after initial skin injury at wounded margins, but increases in dermal fibroblasts [7]. The importance of Cx43 in skin repair is evidenced by the fact that heterozygous Cx43 knockout mice exhibit early wound closure associated with higher proliferation and mobilization of keratinocytes in wound healing [8]. Furthermore, animals treated topically with Cx43 antisense oligodeoxynucleotides display improved closing of skin lesions with significantly lower deposits of granulation tissue and subsequent reduction in scar formation [9]. Likewise, wounded and burned murine skin treated with Cx43 antisense oligodeoxynucleotides presented accelerated wound healing, enhanced keratinocyte proliferation, and increased migration of fibroblasts and more pronounced collagen deposits [5,10]. Lu and group [11] demonstrated that fibroblasts derived from keloids or hypertrophic scars have considerably lower quantities of Cx43 compared with counterparts derived from normal skin. In addition, diabetic rats exhibit delayed wound re-epithelialization and abnormal expression of Cx43 in the epidermis of the wound edges [12]. Altogether, these observations point to a clear-cut role for Cx43 in skin repair. In this context, the present study was set up to further identify the molecular mechanisms related to wound healing affected by Cx43. For this purpose, several parameters, including re-epithelialization, neovascularization, collagen deposition and extracellular matrix remodeling, were monitored over time during experimentally induced skin repair in heterozygous Cx43 knockout mice.

2. Materials and methods

2.1. Animals

Eight-week-old male wild-type (WT, $n = 18$) and heterozygous knockout ($Cx43^{+/-}$, $n = 18$) mice with a CD1 background were used in this study. $Cx43^{+/-}$ mice were obtained from the International Agency for Research on Cancer (France) and were generated by replacing exon 2 of the Cx43 gene with the neomycin resistance gene [13]. Mice were housed under controlled conditions (*i.e.* temperature, 22 ± 2 °C, relative humidity 65 ± 15%, and 12 h light/dark cycle). All mice had access to commercial diet and filtered water *ad libitum*. These management conditions were in accordance with the recommendations of National Research Council (2010) and animal studies were performed with the approval of the Committee on Care and Use of Animal Resources of the School of Veterinary Medicine and Animal Science, University of São Paulo, Brazil (protocol no. 1525008).

2.2. Genotyping

Genotyping was performed according to standard procedures using tail-derived DNA as previously described [14]. Primer pairs used for detection of the endogenous Cx43 gene were 5′-CCCCACTCTCACCTATGTCTCC-3′ and 5′-ACTTTTGCCGCCTAGCTATCCC-3′, generating a polymerase chain reaction (PCR) product of 520 base pair (bp). Primer pairs used for detection of the neomycin resistance

Europe PMC Funders Author Manuscripts

Europe PMC Funders Author Manuscripts

gene were 5′-GGCCACAGTCGATGAATCCAG-3′ and 5′-TATCCATCATGGCTGATGCAA-3′, generating a PCR product of 294 bp. The amplicons were loaded onto a 1.5% agarose gel in Tris-buffered saline.

2.3. Excisional wounding procedures

Excisional punches were made as described previously with slight modification [15]. Mice (±30 g) were anesthetized by intraperitoneal injection of 100 mg/kg ketamine and 20 mg/kg xylazine. Their dorsal skin was cleaned, shaved and sterilized with iodine solution. Two 5 mm full-thickness excisional punches were created through the skin and *panniculus carnosus* on the upper paravertebral region. Wounds were photographed daily and visually monitored for possible signs of infection. The wound areas were standardized by comparison on day *N* with the original wound size on day 0 and expressed as a percentage of wound closure using the formula [(day 0 area - day *N* area)/day 0 area] × 100. The extent of wound contraction was visualized as the edge of scar and was easily distinguishable from the extent of re-epithelialization.

2.4. Histological analysis

Wound beds surrounded by a margin of non-wounded skin were collected at days 3, 7 and 14 post-injury (n = 6/genotype/day). Wounds were divided in half in the least healed portion. Half of the wound was fixed overnight at 4 °C in 60% methanol, 30% chloroform and 10% acetic acid. Tissues were processed through graded ethanol solutions and embedded in paraffin blocks. Tissue sections of 5 μm were stained with hematoxylin/eosin or Sirius red. The other half of the wound was collected in RNAlater (Qiagen, USA), submerged in liquid nitrogen and stored at −80 °C for further analysis.

2.5. Wound re-epithelialization and neovascularization

Hematoxylin/eosin-stained slides were evaluated for the presence of newly formed blood vessels and thickness of the epithelium 3, 7 and 14 days after injury. For the latter, 10 measurements per animal were carried out and averaged, with 5 on each edge of the skin lesion. Quantification of blood vessel formation was performed in 10 wound areas in the dermal region of the lesion. Quantification of collagen deposits during tissue remodeling was performed on Sirius red stained slides. Ten fields in the tissue remodeling area were measured on each slide. The proportion of collagen fibers relative to the total area of remodeling in the dermis after injury was quantified. All analyses were performed using the image analysis Image-Pro Plus system (Media Cybernetics, USA). The average number of newly formed blood vessels was expressed per μm^2 of injured area. The average thickness of the epithelium and the total area of collagen were expressed in mm and percentage, respectively.

2.6. Immunohistochemistry analysis of dermal fibroblast activation and proliferation

For quantification of activation and proliferation of fibroblasts, double immunohistological staining of alpha smooth muscle actin (αSMA) and proliferating cell nuclear antigen (PCNA) was performed. Briefly, histological sections were incubated with primary antibodies raised against αSMA (Sigma, USA; 1:100) and PCNA (Dako, USA; 1:100)

Europe PMC Funders Author Manuscripts

Europe PMC Funders Author Manuscripts

revealed, respectively, by Fast red and Diaminobezidine according to the manufacturer's instructions (EnVision Doublestain System, Dako, USA). Morphometric analysis was performed for the quantification of total fibroblasts and proliferating fibroblasts using an image analysis Image-Pro Plus system (Media Cybernetics, USA). Results were expressed as number of cells per μm^2 of injured tissue.

2.7. Immunofluorescence staining of collagens type I and III

During the early stages of wound healing, fibroblasts actively produce type III collagen. During remodeling, type III collagen is replaced by type I collagen to restore the normal dermal collagen composition [16]. Histological sections were unmasked in Tris–ethylenediaminetetraacetic acid solution at pH 9.0 for 20 min in a microwave at 700 W. Sections were then subjected to enzymatic digestion with 0.4% pepsin (Sigma, USA) diluted in 0.5 N acetic acid for 30 min at 37 °C. Thereafter, sections were subsequently rinsed and incubated overnight in a moisturized chamber at 4 °C with primary antibodies raised against collagen type I or type III (Rockland, USA; 1:50). Next, slides were incubated with secondary antibody swine anti-rabbit IgG, FITC-conjugated (Dako, USA, 1:100). After 90 min incubation in moist and dark chamber, the sections were counterstained with propidium iodide (1:1000), which stains the cell nucleus in red. Finally, slides were mounted with Vectashield (Vector Laboratories, USA), sealed with nail polish and photographed using a Nikon E-800 fluorescence microscope (Nikon, Japan).

2.8. Quantitative real-time PCR analysis

The qPCR technique was performed following the MIQE guidelines [17]. Total RNA (*i.e.* 3 μg) was isolated from skin tissue using the RNAspin mini RNA isolation kit (GE HealthCare, USA) and was reverse transcribed to cDNA using random primers and VILO Master Mix kit (Invitrogen). Primers and probes assays for real-time PCR were purchased from Applied Biosystems (USA), including those for: collagen type I (assay ID Mm00801666_g1), collagen type III (assay ID Mm00802332_m1), transforming growth factor beta 1 (TGFβ-1; assay ID Mm00441724_m1), matrix metallopeptidase 2 (MMP-2; assay ID Mm00439508_m1). 18S rRNA (assay ID Mm04277571_s1) and ACTB (assay ID Mm00607939_s1) were used as reference gene to normalize the results. Each sample was analyzed in duplicate and negative controls were enrolled; its efficiency was verified and established between 95% and 105%. Analyses were carried out using an ABI PRISM 7000 device (Applied Biosystems, USA). Analyses of relative gene expression data were performed according to the $2^{-\Delta\Delta Cq}$ method [18]. Results were expressed as fold change of ΔΔCq values obtained from WT mice at the respective day of measurement.

2.9. Statistical analyses

For all parameters tested, 6 animals per genotype were used. All data were expressed as mean ± standard deviation. Comparison of parameters between different genotypes or groups was performed using analysis of variance with Scheffe's test and paired Student's *t*-tests with 2-tailed comparisons. A *p* value of less than 0.05 indicated a significant difference between experimental groups.

Europe PMC Funders Author Manuscripts

Europe PMC Funders Author Manuscripts

3. Results

3.1. Cx43 deficiency accelerates re-epithelialization and wound closure

Macroscopic analysis of skin wounds showed resolution of edema from day 3 and 5 post-injury onwards in $Cx43^{+/-}$ and WT mice, respectively. Overall, wound healing was improved in $Cx43^{+/-}$ mice compared to their WT counterparts, with less erythema and exsudates on day 5 post-injury and more pronounced wound retraction on day 11 (Fig. 1A). Furthermore, the wound area was significantly reduced in $Cx43^{+/-}$ mice from day 7 onwards (Fig. 1B). In the next series of experiments, measurement of epithelium thickness and quantification of newly formed blood vessels in skin lesions was performed on day 3, 7 and 14 following wounding. Thickening of the epithelium culminated on day 7 in both genotypes, yet significantly higher in $Cx43^{+/-}$ mice, and returned to normal thickness on day 14 in both genotypes (Fig. 2A and B). *De novo* formation of blood vessels was significantly lower on day 3 in $Cx43^{+/-}$ mice, but was similar to that observed in WT animals on day 7 and 14 (Fig. 2C). This was accompanied by greater projections of the epithelium over wounds on day 3 in $Cx43^{+/-}$ mice (Fig. 2A).

3.2. Cx43 deficiency does not affect collagen deposition during wound healing

Progressive increase of collagen production and deposits, revealed by Sirius Red staining, was detected in the dermis during the wound healing period in both test groups (Fig. 3A). Quantification of collagen deposits by morphometric analysis showed no significant difference between $Cx43^{+/-}$ and WT mice (Fig. 3B). In line with this observation, immunostaining of collagen type I and III in the tissue remodeling area indicated upregulated deposition after skin injury occurring to a similar extent in both genotypes. In this analysis, diffuse and disorganized deposits of collagen type I and III were seen in the damaged area on day 3 post-wounding. Accumulation of both collagens in non-patterned dense connective tissue intensified on day 7 and seemed complete on day 14 (Fig. 3C and D).

3.3. Cx43 deficiency increases proliferation and activation of dermal fibroblasts

Evaluation of activation and proliferation of dermal fibroblasts following wounding was accomplished by double immunohistochemical staining of αSMA and PCNA, respectively (Fig. 4A). Quantification of fibroblasts present in the remodeling area showed an increase from day 3 to day 7, followed by a decrease toward day 14 in all animals (Fig. 4B). A similar profile was produced when counting the number of activated (*i.e.* αSMA) and proliferating (*i.e.* PCNA) fibroblasts in the injury area (Fig. 4C). Importantly, at all time points and for all parameters measured, significantly higher values of activated and proliferating fibroblasts were observed for $Cx43^{+/-}$ mice compared to WT animals.

3.4. Cx43 deficiency enhances the expression extracellular matrix remodeling mediators

Gene expression patterns of several mediators of extracellular matrix remodeling were analyzed by qPCR during wound healing. In $Cx43^{+/-}$ mouse skin, mRNA amounts of collagen type I (*p* value 0.008), collagen type III (*p* value 0.025), MMP-2 (*p* value 0.038) and TGFβ-1 (*p* value 0.003) peaked 7 days after skin injury. Gene expression levels returned

to WT baseline levels toward day 14 (Fig. 5). These modifications in transcriptional profiles point to enhanced extracellular matrix remodeling upon Cx43 deficiency.

4. Discussion

Gap junctions were first described in 1967 in liver cells [19,20]. In 1974, Goodenough isolated 2 gap junctional proteins from mouse liver and called them connexins [21]. Gap junctions that connect adjacent cells are composed by two hemichannels, each of which is formed by six proteins named connexins. Gap junctions allow the intercellular diffusion of small molecules (<1–2 kDa), metabolites and secondary messengers such as ions, cAMP and IP3 [22,23]. This flux is called gap junction intercellular communication (GJIC) and is controlled by many mechanisms, including phosphorylation of connexins. Because of the nature of the substances that can diffuse from one cell to another, gap junctions play an important role in regulating tissue homeostasis and different processes responsible for the recovery of this critical balance, triggered as a result of damage such as wound healing and tissue repair, angiogenesis and carcinogenesis [24–27].

Cx43 is an acknowledged goalkeeper of skin homeostasis. Indeed, a number of critical functions have been assigned to Cx43, including roles in the differentiation and migration of both keratinocytes and dermal fibroblasts. Cx43 is equally involved in situations whereby the homeostatic balance in skin is disrupted, such as occurring during wound healing upon skin injury [1–4]. Cx43-deficient mice have proved to be valuable models to investigate the participation of Cx43 in skin physiology and pathology. Since homozygous $Cx43^{-/-}$ die at birth, only heterozygous $Cx43^{+/-}$ animals can be used for research purposes. In the present study, experimentally induced skin repair was induced in $Cx43^{+/-}$ mice and a number of relevant parameters related to wound healing were monitored up to 14 days post-injury. It was found that genetic Cx43 deficiency accelerates re-epithelialization and wound closure, increases proliferation and activation of dermal fibroblasts, and enhances the expression of extracellular matrix remodeling mediators. These results are in line with previous studies in which Cx43 antisense oligodeoxynucleotides were applied on experimentally induced wounds in murine skin tissue [5,9,10]. However, unlike others [10], collagen deposition was not affected in the experimental setting addressed in the current study. It should be mentioned that animal models in which connexin production has been (epi)genetically modified do not allow to distinguish between gap junction and hemichannel activity. Connexin hemichannels have long been considered as merely structural precursors, yet compelling evidence in the last few years clearly shows that hemichannels autonomously form a pathway of communication, albeit not between neighboring cells, as is the case for gap junctions, but between the cytosol of individual cells and their extracellular environment. In fact, not only dysregulated gap junctional communication, but also aberrant connexin hemichannel activity has been observed in a number of skin diseases [28–31]. Several authors have reported Cx43 modulation in human diseases related to poor skin healing, such as hypertrophic scars and keloids [11] or in wounds of diabetic patients [32,33]. Fibroblasts derived from keloid or hypertrophic scars indeed have much smaller amount of Cx43 in comparison with normal skin. This indicates that GJIC is important for controlling the balance between proliferation and apoptosis of fibroblasts in the skin, as well as for managing the production of ECM [11]. Great promise, therefore, lies in the

Europe PMC Funders Author Manuscripts
Europe PMC Funders Author Manuscripts

Europe PMC Funders Author Manuscripts

Europe PMC Funders Author Manuscripts

pharmacological inhibition of connexin signaling for the clinical management of skin disorders. In this context, Gap27, a peptide that reproduces an amino acid sequence of the second extracellular loop of Cx43, has been repeatedly reported to improve skin wound healing. Gap27 hereby blocks both Cx43-mediated gap junctional [34] and hemichannel [6] activity, and increases proliferation and migration rates of keratinocytes and dermal fibroblasts [6,34]. Moreover, Gap27 upregulates genes associated with extracellular matrix remodeling [35], which is reminiscent of our observations. Collectively, these reports thus demonstrate that Cx43 signaling represents a promising therapeutic target in wound healing, a finding that is clearly underscored by the results of the present study.

Acknowledgements

This work was financially supported by the grants of the 'Fundação de Auxílio à Pesquisa do Estado de São Paulo' (FAPESP grant 07/59764-9 and SPEC FAPESP grant 13/50420-6) and the European Research Council (Starting Grant 335476).

References

[1]. Becker DL, Thrasivoulou C, Phillips AR. Connexins in wound healing; perspectives in diabetic patients. Biochim Biophys Acta. 2012; 1818:2068–75. [PubMed: 22155211]

[2]. Scott CA, Tattersall D, O'Toole EA, Kelsell DP. Connexins in epidermal homeostasis and skin disease. Biochim Biophys Acta. 2012; 1818:1952–61. [PubMed: 21933662]

[3]. Churko JM, Laird DW. Gap junction remodeling in skin repair following wounding and disease. Physiology. 2013; 28:190–8. [PubMed: 23636264]

[4]. Martin PE, Easton JA, Hodgins MB, Wright CS. Connexins: sensors of epidermal integrity that are therapeutic targets. FEBS Lett. 2014; 588:1304–14. [PubMed: 24607543]

[5]. Coutinho P, Qiu C, Frank S, Wang CM, Brown T, Green CR, et al. Limiting burn extension by transient inhibition of connexin 43 expression at the site of injury. Br J Plast Surg. 2005; 58:658–67. [PubMed: 15927148]

[6]. Pollok S, Pfeiffer AC, Lobmann R, Wright CS, Moll I, Martin PE, et al. Connexin 43 mimetic peptide Gap27 reveals potential differences in the role of Cx43 in wound repair between diabetic and non-diabetic cells. J Cell Mol Med. 2011; 15:861–73. [PubMed: 20345849]

[7]. Brandner JM, Houdek P, Hüsing B, Kaiser C, Moll I. Connexins 26, 30, and 43: differences among spontaneous, chronic, and accelerated human wound healing. J Investig Dermatol. 2004; 122:1310–20. [PubMed: 15140236]

[8]. Kretz M, Euwens C, Hombach S, Eckardt D, Teubner B, Traub O, et al. Altered connexin expression and wound healing in the epidermis of connexin-deficient mice. J Cell Sci. 2003; 116:3443–52. [PubMed: 12840073]

[9]. Qiu C, Coutinho P, Frank S, Franke S, Law LY, Martin P, et al. Targeting connexin 43 expression accelerates the rate of wound repair. Curr Biol. 2003; 13:1697–703. [PubMed: 14521835]

[10]. Mori R, Power KT, Wang CM, Martin P, Becker DL. Acute downregulation of connexin 43 at wound sites leads to a reduced inflammatory response, enhanced keratinocyte proliferation and wound fibroblast migration. J Cell Sci. 2006; 119:5193–203. [PubMed: 17158921]

[11]. Lu F, Gao J, Ogawa R, Hyakusoku H. Variations in gap junctional intercellular communication and connexin expression in fibroblasts derived from keloid and hypertrophic scars. Plast Reconstr Surg. 2007; 119:844–51. [PubMed: 17312486]

[12]. Wang CM, Lincoln J, Cook JE, Becker DL. Abnormal connexin expression underlies delayed wound healing in diabetic skin. Diabetes. 2007; 56:2809–17. [PubMed: 17717278]

[13]. Reaume AG, de Sousa PA, Kulkarni S, Langille BL, Zhu D, Davies TC, et al. Cardiac malformation in neonatal mice lacking connexin 43. Science. 1995; 267:1831–4. [PubMed: 7892609]

Europe PMC Funders Author Manuscripts

Europe PMC Funders Author Manuscripts

[14]. Cogliati B, Da Silva TC, Aloia TP, Chaible LM, Real-Lima MA, Sanches DS, et al. Morphological and molecular pathology of CCL4-induced hepatic fibrosis in connexin 43-deficient mice. Microsc Res Tech. 2011; 74:421–9. [PubMed: 20830702]

[15]. Birch M, Tomlinson A, Ferguson MW. Animal models for adult dermal wound healing. Methods Mol Med. 2005; 117:223–35. [PubMed: 16118455]

[16]. Madden JW, Peacock EE. Studies on the biology of collagen during wound healing. Rate of collagen synthesis and deposition in cutaneous wounds in the rat. Surgery. 1968; 64:288–94. [PubMed: 5658731]

[17]. Bustin SA, Benes V, Garson JA, Hellemans J, Huggett J, Kubista M, et al. The MIQE guidelines: minimum information for publication of quantitative real-time PCR experiments. Clin Chem. 2009; 55:611–22. [PubMed: 19246619]

[18]. Livak KJ, Schmittgen TD. Analysis of relative gene expression data using real-time quantitative PCR and the 2(−Delta Delta C(T)) method. Methods. 2001; 25:402–8. [PubMed: 11846609]

[19]. Loewenstein WR, Kanno Y. Intercellular communication and tissue growth. I. Cancerous growth. J Cell Biol. 1967; 33:225–34. [PubMed: 6039367]

[20]. Revel JP, Karnovsky MJ. Hexagonal array of subunits in intercellular junctions of the mouse heart and liver. J Cell Biol. 1967; 33:C7–12. [PubMed: 6036535]

[21]. Goodenough DA. Bulk isolation of mouse hepatocyte gap junctions. Characterization of the principal protein, connexin. J Cell Biol. 1974; 61:557–63. [PubMed: 4363961]

[22]. Yamasaki H, Naus CC. Role of connexin genes in growth control. Carcinogenesis. 1996; 17:1199–213. [PubMed: 8681433]

[23]. Willecke K, Hennemann H, Dahl E, Jungbluth S, Heynkes R. The diversity of connexin genes encoding gap junctional proteins. Eur J Cell Biol. 1999; 1:1–7.

[24]. Yamasaki H. Role of disrupted gap junctional intercellular communication in detection and characterization of carcinogens. Mutat Res. 1996; 365:91–105. [PubMed: 8898991]

[25]. Trosko JE, Ruch RJ. Cell–cell communication in carcinogenesis. Front Biosci. 1998; 3 d208ÿd236.

[26]. Trosko JE, Ruch RJ. Gap junctions as targets for cancer chemoprevention and chemotherapy. Curr Drug Targets. 2002; 3:465–82. [PubMed: 12448698]

[27]. Chanson M, Derouette JP, Roth I, Foglia B, Scerri I, Dudez T, et al. Gap junctional communication in tissue inflammation and repair. Biochim Biophys Acta. 2005; 1711:197–207. [PubMed: 15955304]

[28]. Essenfelder GM, Bruzzone R, Lamartine J, Charollais A, Blanchet-Bardon C, Barbe MT, et al. Connexin30 mutations responsible for hydrotic ectodermal dysplasia cause abnormal hemichannel activity. Hum Mol Genet. 2004; 13:1703–14. [PubMed: 15213106]

[29]. Gerido DA, DeRosa AM, Richard G, White TW. Aberrant hemichannel properties of Cx26 mutations causing skin disease and deafness. Am J Physiol Cell Physiol. 2004; 293:C337–45. [PubMed: 17428836]

[30]. Mese G, Sellitto C, Li L, Wang HZ, Valiunas V, Richard G, et al. The Cx26-G45E mutation displays increased hemichannel activity in a mouse model of the lethal form of keratitis-ichthyosis-deafness syndrome. Mol Biol Cell. 2011; 22:4776–86. [PubMed: 22031297]

[31]. Mhaske PV, Levit NA, Li L, Wang HZ, Lee JR, Shuja Z, et al. The human Cx26-D50A and Cx26-A88V mutations causing keratitis-ichthyosis-deafness syndrome display increased hemichannel activity. Am J Physiol Cell Physiol. 2013; 304:C1150–58. [PubMed: 23447037]

[32]. Abdullah KM, Luthra G, Bilski JJ, Abdullah SA, Reynolds LP, Redmer DA, et al. Cell-to-cell communication and expression of gap junctional proteins in human diabetic and nondiabetic skin fibroblasts: effects of basic fibroblast growth factor. Endocrine. 1999; 10:35–41. [PubMed: 10403569]

[33]. Bajpai S, Shukla VK, Tripathi K, Srikrishna S, Singh RK. Targeting connexin 43 in diabetic wound healing: future perspectives. J Postgrad Med. 2009; 55:143–9. [PubMed: 19550065]

[34]. Wright CS, van Steensel MA, Hodgins MB, Martin PE. Connexin mimetic peptides improve cell migration rates of human epidermal keratinocytes and dermal fibroblasts *in vitro*. Wound Repair Regen. 2009; 17:240–9. [PubMed: 19320893]

[35]. Wright CS, Pollok S, Flint DJ, Brandner JM, Martin PE. The connexin mimetic peptide Gap27 increases human dermal fibroblast migration in hyperglycemic and hyperinsulinemic conditions *in vitro*. J Cell Physiol. 2012; 227:77–87. [PubMed: 21984074]

Europe PMC Funders Author Manuscripts

Europe PMC Funders Author Manuscripts

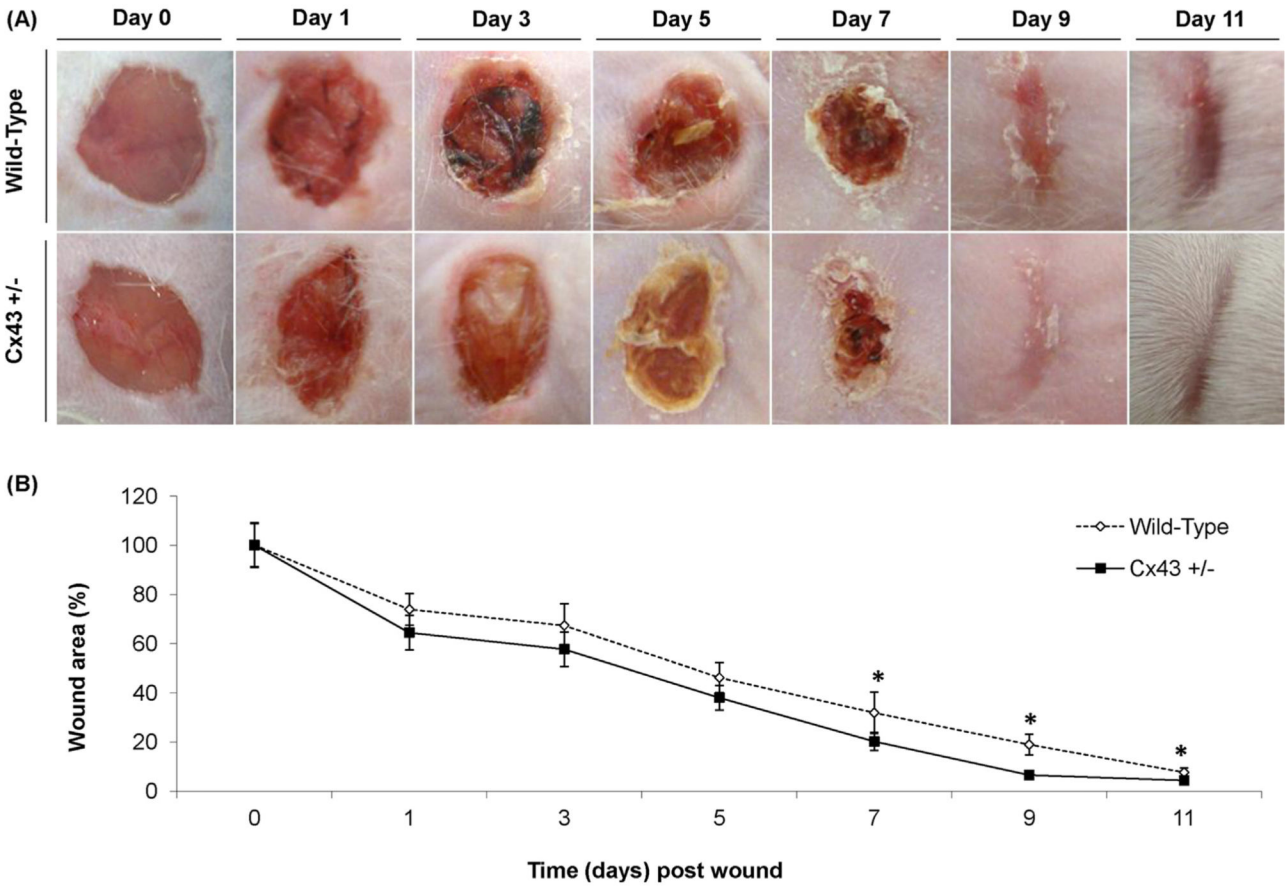

Fig. 1.

Macroscopic evaluation (A) and morphometric analysis (B) of the lesion area 0, 1, 3, 5, 7, 9 and 11 days after skin wounding in WT and $Cx43^{+/-}$ mice (n = 36).

Europe PMC Funders Author Manuscripts

Europe PMC Funders Author Manuscripts

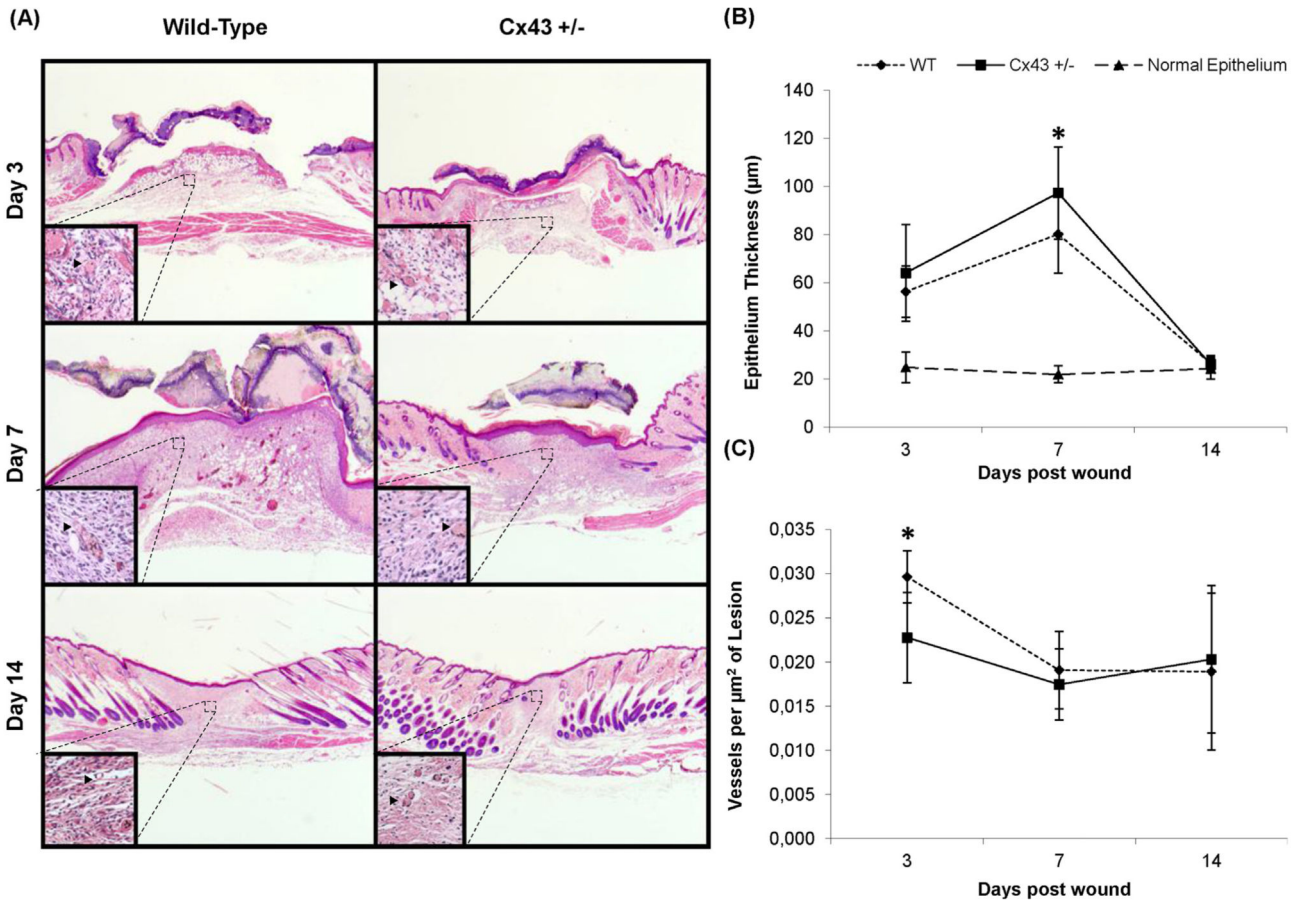

Fig. 2.

Hematoxylin/eosin-stained lesions (A), re-epithelialization (B) and neovascularization (arrowheads), in WT and $Cx43^{+/-}$ mice 3, 7 and 14 days after skin wounding. *$p < 0.05$ (n = 6 per genotype). Vessels are highlighted in the details (head).

Europe PMC Funders Author Manuscripts
Europe PMC Funders Author Manuscripts

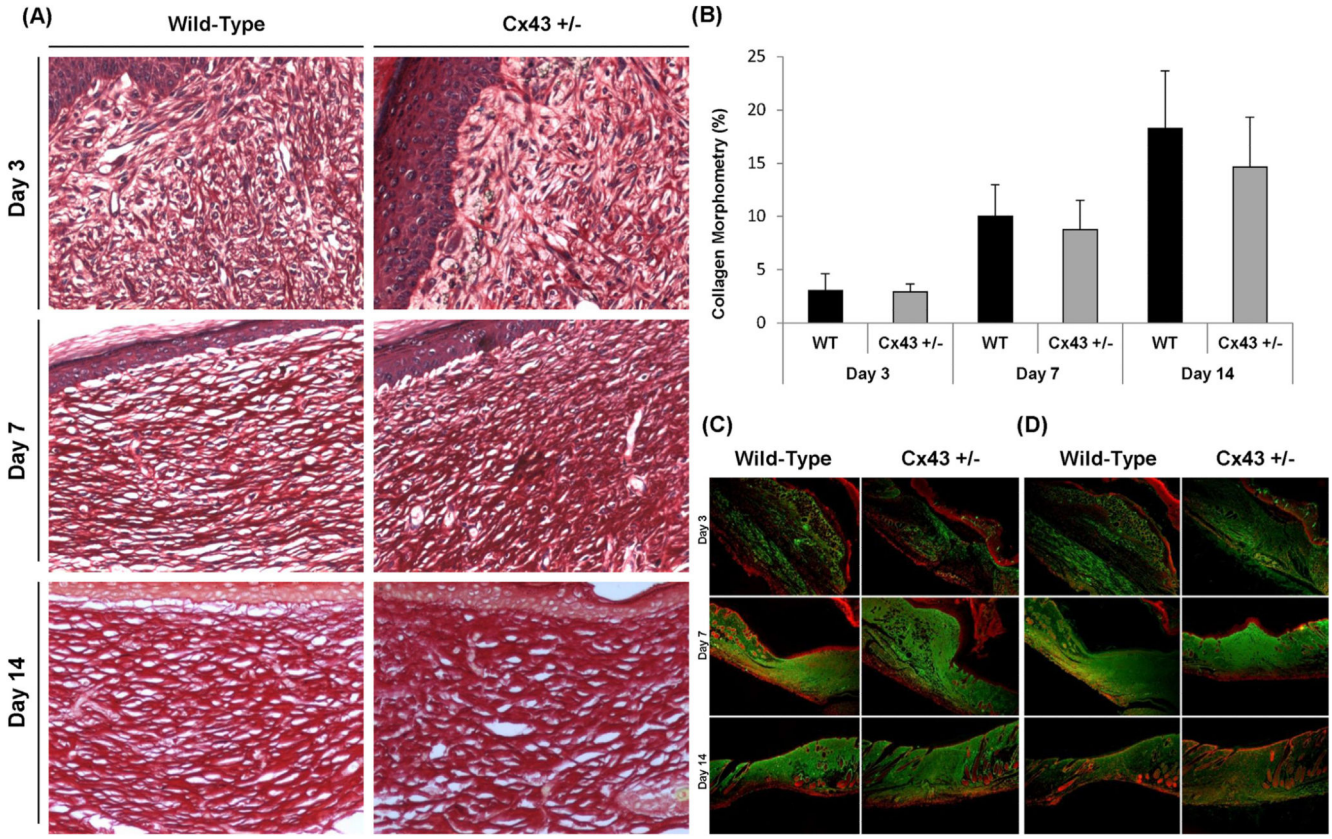

Fig. 3.

Picro Sirius red staining of collagen deposition at 40× magnification (A), morphometric analysis of collagen deposits (B) and immunostaining (green) of collagen type I (C) and III (D) with nuclear counterstaining (red) at 40× magnification in WT and $Cx43^{+/-}$ mice 3, 7 and 14 days after skin wounding. * $p < 0.05$ ($n = 6$ per genotype).

Europe PMC Funders Author Manuscripts
Europe PMC Funders Author Manuscripts

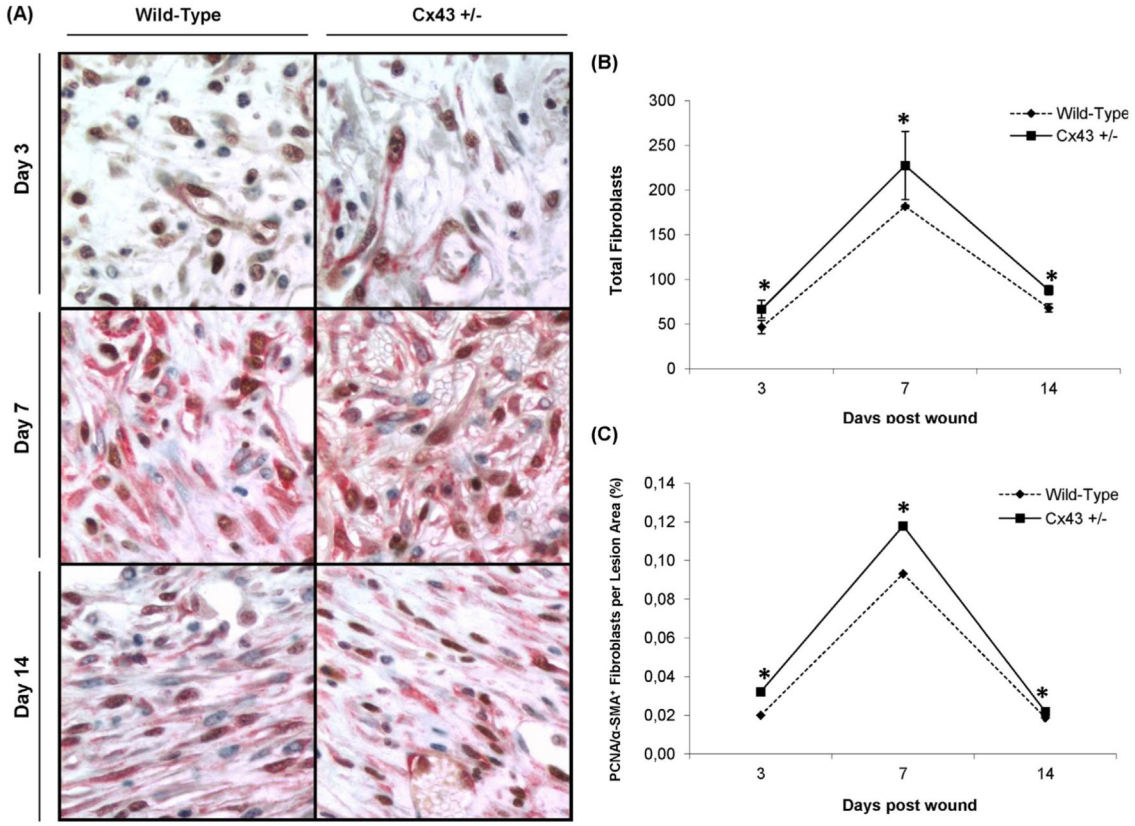

Fig. 4.

Double immunohistological staining of αSMA (red) and PCNA (brown) at 400× magnification (A), quantification of the total number fibroblasts (B) and the number of fibroblasts positive for PCNA and αSMA in the lesion area in WT and Cx43$^{+/-}$ mice 3, 7 and 14 days after skin wounding. *$p < 0.05$ ($n = 6$ per genotype).

Europe PMC Funders Author Manuscripts
Europe PMC Funders Author Manuscripts

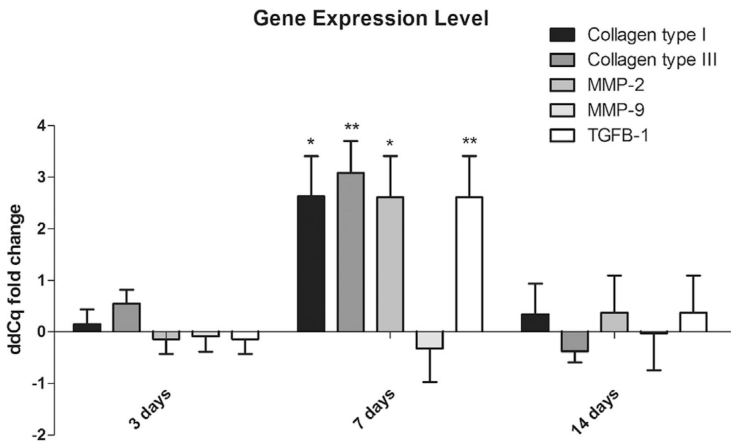

Fig. 5.

Changes in gene expression of collagen type I and III, TGFβ-1, MMP-2 and MMP-9 in WT and $Cx43^{+/-}$ mice 3, 7 and 14 days after skin wounding. The bars showing the average of ΔΔCq of $Cx43^{+/-}$ mice normalized by WT animals, with the respective SEM. *$p < 0.05$ and **$p < 0.01$ ($n = 6$ per genotype).

Europe PMC Funders Author Manuscripts

Europe PMC Funders Author Manuscripts